Conversion of Commensal *Escherichia coli* K-12 to an Invasive Form via Expression of a Mutant Histone-Like Protein

Preeti Koli,[a] Sudhanshu Sudan,[a] David Fitzgerald,[b] Sankar Adhya,[b] and Sudeshna Kar[a]

Institute of Molecular Medicine, New Delhi, India,[a] and Laboratory of Molecular Biology, National Cancer Institute, National Institutes of Health, Bethesda, Maryland, USA[b]

ABSTRACT **The HU$\alpha^{E38K, V42L}$ mutant of the bacterial histone-like protein HU causes a major change in the transcription profile of the commensal organism *Escherichia coli* K-12 (Kar S, Edgar R, Adhya S, Proc. Natl. Acad. Sci. U. S. A. 102:16397–16402, 2005). Among the upregulated genes are several related to pathogenic interactions with mammalian cells, as evidenced by the expression of curli fibers, Ivy, and hemolysin E. When *E. coli* K-12/ HU$\alpha^{E38K, V42L}$ was added to Int-407 cells, there was host cell invasion, phagosomal disruption, and intracellular replication. The invasive trait was also retained in a murine ileal loop model and intestinal explant assays. In addition to invasion, the internalized bacteria caused a novel subversion of host cell apoptosis through modification and regulation of the BH3-only proteins Bim_{EL} and Puma. Changes in the transcription profile were attributed to positive supercoiling of DNA leading to the altered availability of relevant promoters. Using the *E. coli* K-12/ HU$\alpha^{E38K, V42L}$ variant as a model, we propose that traditional commensal *E. coli* can adopt an invasive lifestyle through reprogramming its cellular transcription, without gross genetic changes.**

IMPORTANCE ***Escherichia coli* K-12 is well established as a benign laboratory strain and a human intestinal commensal. Recent evidences, however, indicate that the typical noninvasive nature of resident *E. coli* can be reversed under specific circumstances even in the absence of any major genomic flux. We previously engineered an *E. coli* strain with a mutant histone-like protein, HU, which exhibited significant changes in nucleoid organization and global transcription. Here we showed that the changes induced by the mutant HU have critical functional consequences: from a strict extracellular existence, the mutant *E. coli* adopts an almost obligate intracellular lifestyle. The internalized *E. coli* exhibits many of the prototypical characteristics of traditional intracellular bacteria, like phagosomal escape, intracellular replication, and subversion of host cell apoptosis. We suggest that *E. coli* K-12 can switch between widely divergent lifestyles in relation to mammalian host cells by reprogramming its cellular transcription program and without gross changes in its genomic content.**

Received 16 August 2011 **Accepted** 17 August 2011 **Published** 6 September 2011

Citation Koli P, Sudan S, Fitzgerald D, Adhya S, Kar S. 2011. Conversion of commensal *Escherichia coli* K-12 to an invasive form via expression of a mutant histone-like protein. mBio 2(5):e00182-11. doi:10.1128/mBio.00182-11.

Editor B. Brett Finlay, The University of British Columbia

Address correspondence to Sankar Adhya, sadhya@helix.nih.gov, or Sudeshna Kar, sudeshnak@immindia.org.

The status of *Escherichia coli* K-12, arguably the most completely characterized single-cell life form, as a noninvasive laboratory-adapted strain of bacteria and a benign commensal of the human gut is well entrenched. By virtue of its lack of sophisticated virulence machinery, its stringent negative regulation of incipient virulence factors, and a lack of evidence for invasive or virulent modes of behavior under diverse host or laboratory conditions tested thus far, there has never been any serious challenge to *E. coli* K-12's standing as an extracellular commensal. The few occasions where K-12 strains have been shown to invade cultured mammalian cells were under conditions of overexpression of bacterial amyloid adhesion factors or heterologous expression of foreign invasive loci (1, 2). However, the cryptic maintenance of classical virulence genes in a traditionally nonpathogenic bacterium like *E. coli* K-12 and spontaneous expression of many of these virulence determinants inside the mammalian hosts (3–5) lead to the intriguing possibility that, under certain specific host conditions, even well-established extracellular commensals can switch to an actively invasive or pathogenic lifestyle, without any major genomic flux. Commensal *E. coli*, the most abundant facultative anaerobe present in the human intestine, is recovered from many extraintestinal locations during disease states (6–8). There have even been reports of an *E. coli* probiotic strain, Nissle 1917, causing severe sepsis (9), leading credence to the view that host niches for resident *E. coli* are not always rigidly defined. The prevailing notion is that either intestinal bacterial overgrowth or a gross breach of intestinal barrier function leads to passive translocation and systemic spread of intestinal *E. coli* (10, 11). Due to the stringent negative regulation of virulence determinants in commensals under normal conditions and our lack of understanding of within-host dynamics of the microbe-host relationship under atypical conditions, the possibility of an alternative host-microbe interaction for traditional commensals has not been explored to a great extent. Uncovering molecular strategies by which commensal *E. coli* can adopt an invasive lifestyle and the physiological impact on host homeostasis can potentially provide a paradigm shift in the standard concepts of the resident microbe-host relationship with regard to virulence and commensalism.

We previously isolated and characterized a gain-of-function mutant of the bacterial histone-like protein HU, HU$\alpha^{E38K,\ V42L}$, which transformed the loosely organized nucleoid of *E. coli* K-12 into a condensed conformation (12, 13). The nucleoid remodeling was accompanied by major changes in the transcription program of the mutant bacterium (SK3842), resulting in dramatic changes in its morphology, physiology, and metabolism. Many of the changes in SK3842 (rod-to-coccoid morphological conversion, altered carbon utilization capabilities, and expression of cryptic virulence genes) were typical of some distinctive traits shown by commensal *E. coli* inside mammalian hosts, indicating a possible deviation from the typical *E. coli* K-12 behavior. Here we explore the mechanism by which HU$\alpha^{E38K,\ V42L}$ activates silent, pathogenicity-linked genes. We also characterize how the resulting physiology allows the mutant to interact "productively" with intestinal epithelial cells. The mutant serves as an *in vitro* locked-in model representing an alternate lifestyle that can be adopted by *E. coli* K-12 without gross genomic changes.

RESULTS

Mechanism of expression of pathogenicity-associated genes. Previous biochemical and structural studies have demonstrated that DNA can wrap around wild-type HU multimers in a left-handed fashion, like histones in eukaryotes, generating negative superhelicity (13). We have also shown that a mutant HUα, HU$\alpha^{E38K,\ V42L}$, multimer forms a right-handed spiral which generates positive superhelicity (14). Moreover, plasmid DNA extracted from wild-type *E. coli* is negatively supercoiled, but it is positively supercoiled when isolated from the mutant HU strain, SK3842 (13). It is commonly believed that the nature and amount of template DNA superhelicity dictate the functional efficiency of promoters (15). We surmised that the global change in the transcription profile in SK3842 is created by a change in the nature and extent of chromosomal superhelicity in the mutant. Our working model assumes that many pathogenicity-linked genes which are expressed only in SK3842 are transcribed because their promoters are available for transcription only when positively supercoiled. We tested this basic idea by studying the transcription of two representative genes having opposite transcription profiles in the wild type and in SK3842 *in vivo*: (i) the *lac* promoter, which is active in the wild type but not in the mutant, and (ii) the *hlyE* promoter (associated with pathogenicity), which behaves in the opposite manner. As expected, an *in vitro* transcription assay using negatively supercoiled DNA template showed that the *lac* promoter was active in the presence of cAMP and its receptor protein (CRP). The presence of HUα did not affect *lac* transcription in a significant way. However, addition of the purified HU$\alpha^{E38K,\ V42L}$ protein turned off not only *lac* transcription but also transcription from the control promoter, *RNA1* (Fig. 1A). We used S-30 extract from a Δ*hupAB* strain for transcription of the *hlyE* promoter since standard *in vitro* transcription mix was not sufficient for its activity. Transcription from the *hlyE* promoter *in vitro* occurred very poorly with negatively supercoiled DNA template but became very active in the presence of HU$\alpha^{E38K,\ V42L}$ (Fig. 1A). These results clearly demonstrate that the differential effect of the HU$\alpha^{E38K,\ V42L}$ mutation on gene expression occurs directly at the promoters of the affected genes. We believe that HU$\alpha^{E38K,\ V42L}$ introduces segments of positive supercoiling into the plasmid DNA, allowing the *hlyE* promoter to become active. This was confirmed by using a *hlyE* promoter-containing plasmid, which was extracted and purified from SK3842 and shown to be positively supercoiled, for transcription. This template allowed a significant level of transcription from the *hlyE* promoter without the addition of any HU protein. Whereas the addition of wild-type HUα increased *hlyE* transcription marginally, addition of HU$\alpha^{E38K,\ V42L}$ increased *hlyE* transcription to a severalfold-higher level (Fig. 1B). Our results strongly suggest that expression of normally silent, pathogenicity-associated genes in *E. coli* requires positively supercoiled DNA.

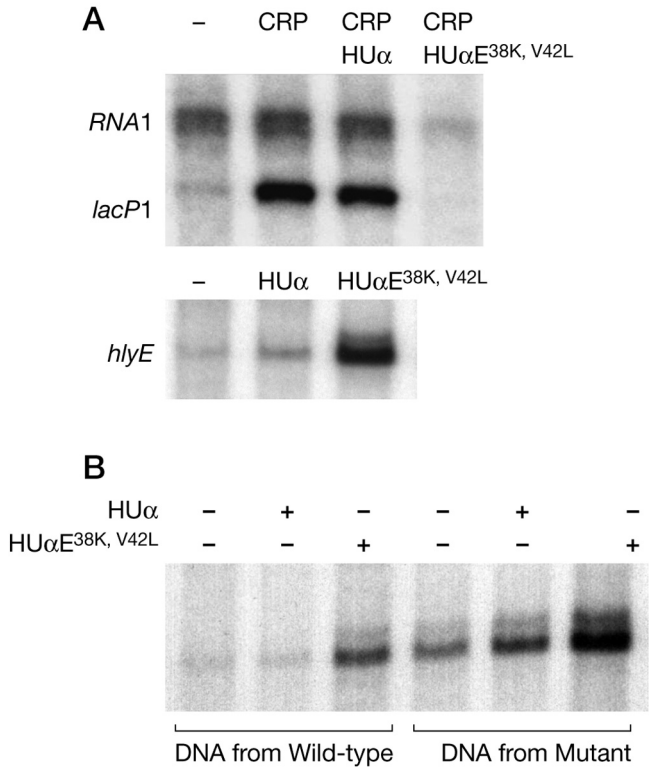

FIG 1 Activation of silent pathogenicity-associated promoters by HU$\alpha^{E38K,\ V42L}$. (A) Differential effect of HU$\alpha^{E38K,\ V42L}$ on *lac* and *hlyE* promoters *in vitro*. Transcription from *lac* (top panel) and *hlyE* (bottom panel) promoters in the presence of HUα and HU$\alpha^{E38K,\ V42L}$ was assayed. Transcription of *lacP* was carried out in standard transcription reaction mix, while *hlyE* transcription was done in the presence of S-30 protein lysate from MG1655 (Δ*hupAB*). (B) HU$\alpha^{E38K,\ V42L}$-induced change in *hlyE* promoter architecture. Plasmid SK302(*hlyE*), containing the *hlyE* promoter, was isolated from MG1655 and SK3842 and used for the transcription assay using an S-30 cell-free transcription system in the absence or presence of either the wild-type HUα or HU$\alpha^{E38K,\ V42L}$ protein.

Invasion of intestinal epithelial cells by SK3842. Since SK3842 demonstrated a dramatically altered gene expression profile, we undertook an investigation of its interaction with mammalian cells. Using transmission electron microscopy (TEM), we characterized the interaction of SK3842 with intestinal epithelial cells (Int-407). SK3842 efficiently invaded Int-407 cells, while the parental K-12 strain, MG1655, remained noninvasive (Fig. 2A). Within 1 h postinfection, there were numerous SK3842 cells enclosed in endocytotic vacuoles. TEM revealed that there were multiple membrane extensions from the surface of the epithelial cells (Fig. 2Bi) and many of the adhering bacteria were surrounded and engulfed by these protrusions (Fig. 2Bii), leading to the internal-

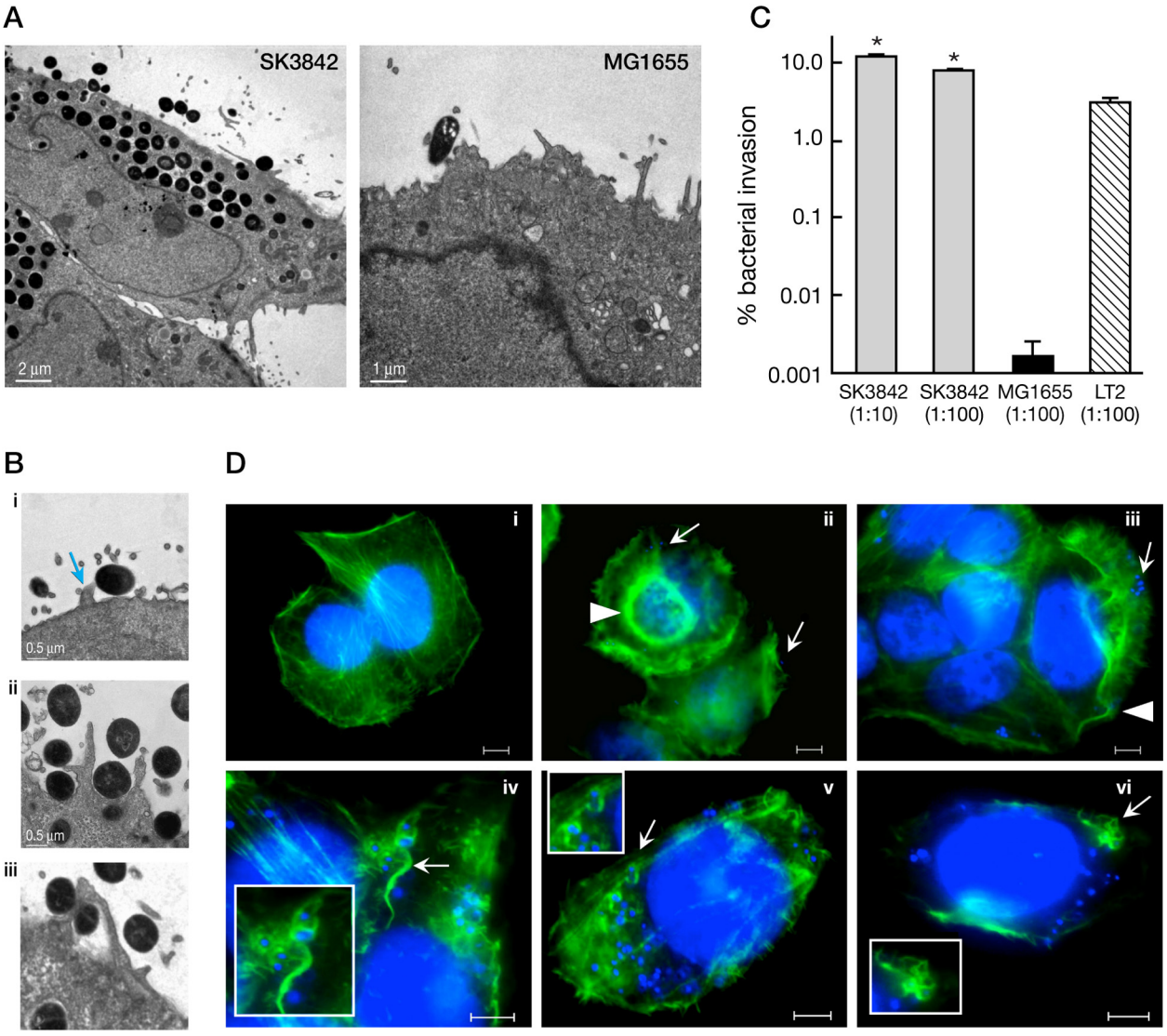

FIG 2 Invasion of intestinal epithelial cells by histone-modified *E. coli* strain SK3842. (A) Internalization of SK3842 in host epithelial cells. TEM of Int-407 cells infected with SK3842 (a) or MG1655 (b) at an MOI of 100 was done. (B) Attachment and entry process. TEM of Int-407 cells infected with SK3842 showing different stages of invasion. (i) Small membrane projections (arrow) on the host cell surface near the point of SK3842 attachment. (ii) Membrane protrusions extending from either side of the anchored bacteria. (iii) Membrane protrusions fuse to engulf the attached bacteria in a membrane-bound vacuole. (C) Invasion efficiency. Int-407 cells were infected with SK3842, MG1655, and LT2, followed by gentamicin treatment. "*" denotes a P value of <0.01 compared to results for MG1655. (D) Reorganization of host cytoskeleton in response to SK3842. Int-407 cells were incubated in the presence of DAPI-stained SK3842 for 0 min (i), 5 min (ii), 10 min (iii), and 30 min (iii to vi). Infected Int-407 cells were labeled with Alexa 488-phalloidin and viewed under a fluorescence microscope. Images show a representative group of cells at the indicated time points. The scale bar represents 5 μm. (i) Control cell. (ii) Arrowhead shows circular dorsal ruffle, and arrows show SK3842 cells. (iii) Arrowhead shows thinner peripheral ruffle, and arrow shows SK3842 cells near ruffled region. (iv) Arrow shows membrane ruffle in close contact with SK3842. (v) Arrow shows loose, actin-rich ruffles forming around SK3842 cells. (vi) Arrow points to tight endocytic cups surrounding SK3842 cells. Inset images in panels iv to vi show magnified images of the association of SK3842 cells with host cell surface structures during the process of entry.

ization of SK3842 in prominent vacuoles (Fig. 2Biii). Using a gentamicin protection assay, we assessed the kinetics of cell invasion at different multiplicities of infection (MOIs). The mean invasive efficiency was 7.46% ± 0.492% with an MOI of 100 and 12.9% ± 1.003% with an MOI of 10 (Fig. 2C). As expected, MG1655 was noninvasive ($P = 0.001$). Remarkably, the invasion efficiency of SK3842 was higher than that of *Salmonella enterica* LT2, an enteric invasive pathogen used as a positive control ($P = 0.009$). Sequences of the bacterial entry event were further analyzed by fluorescence microscopy of Int-407 cells at different time points following the addition of 4[prime],6-diamidino-2-phenylindole (DAPI)-labeled SK3842 (Fig. 2D). Immediately following the addition of SK3842, large, prominent, circular dorsal ruffles were seen on the surface of the host cells (Fig. 2Dii), indicating a rapid reorganization of the cytoskeletal network in contrast to observations for control cells (Fig. 2Di). The large dorsal ruffles were transient in nature and gave way to smaller peripheral ruffles. SK3842 cells accumulated markedly in the ruffled region of the

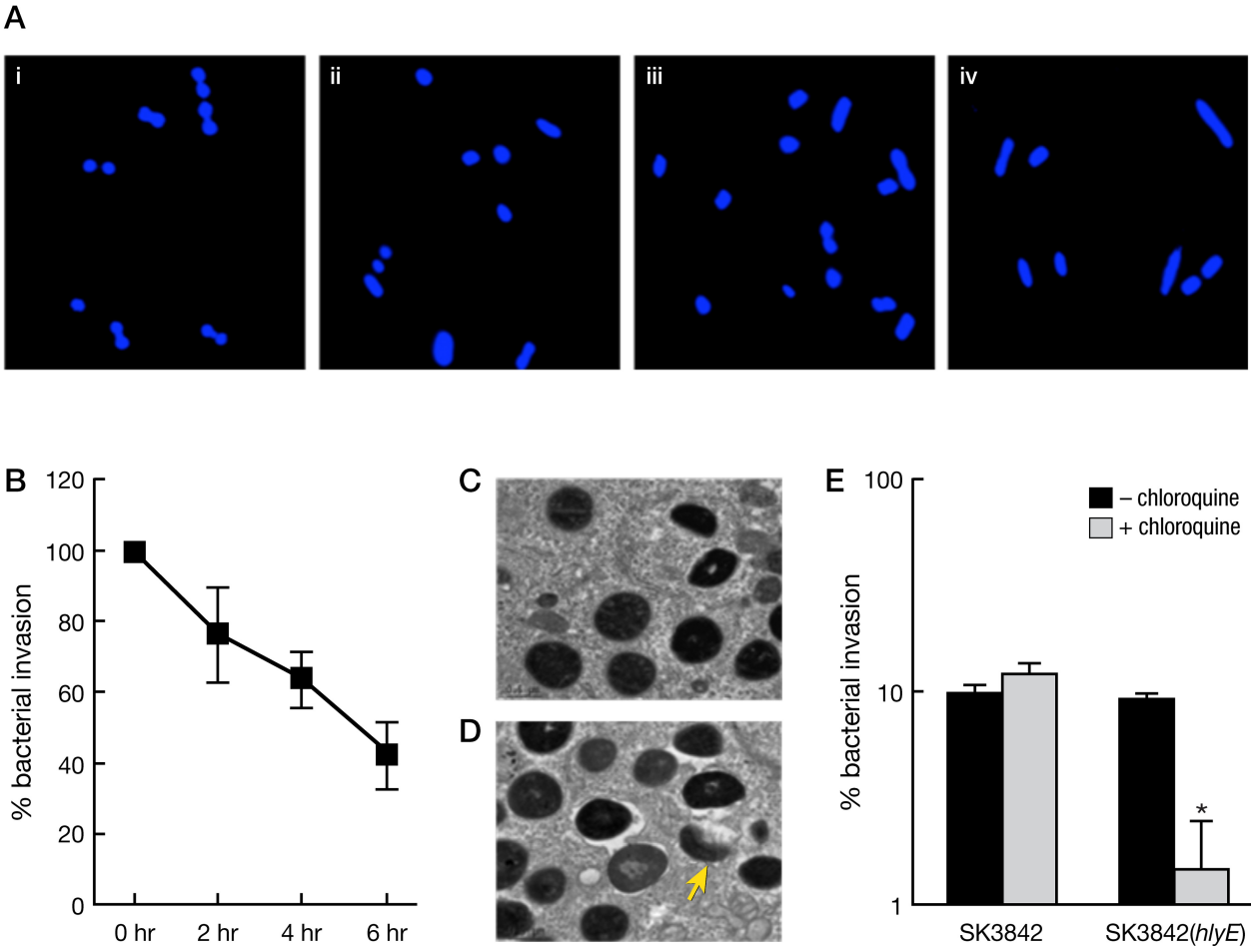

FIG 3 Invasive property of SK3842 is directly coupled to its mutant-HU-related altered characteristics. (A) Reversion of SK3852 to wild-type form by overexpression of wild-type HUα. SK3842 transformed with expression plasmid pWTHU carrying the wild-type HUα gene was induced with IPTG. At 0 min (i), 2 h (ii), 4 h (iii), and 6 h (iv), samples of the induced culture were taken out, stained with DAPI, and visualized under a fluorescence microscope. (B) Invasion efficiency of reverted SK3842 culture. Samples of SK3842(pWTHU) culture at the indicated time points (see panels Ai to Aiv) were used to infect Int-407 cells, and their invasion efficiency was expressed as a percentage of internalization efficiency of the control SK3842 culture transformed with a vector plasmid (100%) at equivalent time points. (C) Escape of SK3842 from endocytic vacuoles. TEM of Int-407 cells infected with SK3842 at a postinvasion time of 6 h. (D) Loss of phagosomal escape in hemolysin-negative SK3842. TEM of *hlyE*-deleted SK3842 inside the host cell 24 h postinvasion was done. The arrowhead points to some of the vacuole-wrapped bacteria in the process of degradation. (E) Quantitative assay of phagosomal escape. Infected Int-407 cells were incubated in the presence of gentamicin or gentamicin plus chloroquine. At 2 h postinfection, cells were lysed and surviving bacteria were enumerated. Percent bacterial invasion in cultures treated with only gentamicin represents total intracellular bacteria. Bacteria recovered in the presence of both gentamcin and chloroquine represent the bacterial population which escaped from vacuoles into the cytosol. "*" denotes a *P* value of <0.001 compared to results for the corresponding SK3842(Δ*hlyE*) strain.

host cell membrane (Fig. 2Diii). SK3842 cells were initially found to be closely apposed to the longer, wavy, membrane ruffles on the host cell surface (Fig. 2Div). Following this, smaller, actin-rich ruffles were seen to form loose, individual associations with the attached SK3842 cells (Fig. 2Dv). Ultimately, these encircling ruffles formed tight endocytic cups enclosing the bacterial cells, leading to their internalization (Fig. 2Dv). This shows that SK3842 induces rapid, reversible, and extensive rearrangement of the host cytoskeletal network prior to and during the process of its entry.

Invasion is a direct and reversible consequence of HU$\alpha^{E38K, V42L}$ expression. Previously we reported that the mutant phenotype of SK3842 can be rescued completely by overexpression of wild-type HUα (12). We used SK3842 carrying a wild-type HUα plasmid [SK382(pWTHU)] and induced wild-type HUα for various lengths of time to obtain cultures with different proportions of wild-type and mutant cells, ranging from 100% mutant (time zero) to 10 to 20% mutant (time 6 h postinduction). Following isopropyl-β-D-thiogalactopyranoside (IPTG) induction, the majority of the spherical SK3842(pWTHU) bacterial cells (time zero; Fig. 3Ai) assumed a larger ovoid shape (time 2 h; Fig. 3Aii), which then converted to short rods (time 4 h; Fig. 3Aiii) and finally to full-length rods (time 6 h; Fig. 3Aiv). Corresponding to the morphological conversion of spheres to rods, there was a time-dependent decline in the invasive ability of SK3842(pWTHU), lowering to 42.3% ± 9.5% of that of the control SK3842 culture after 6 h of IPTG induction (Fig. 3B). This result demonstrates that the invasive property of SK3842 is directly linked to the expression of HU$\alpha^{E38K, V42L}$ and is reversible by overexpression of wild-type HUα.

Escape of SK3842 from endosomes/phagosomes is *hlyE* dependent. For successful survival inside host cells, the internalized bacteria need to escape quickly from the phagosomes or modify

the phagosomes to prevent the formation of phagolysosomes. TEM revealed that the majority of intracellular SK3842 bacteria were free in the host cytosol 6 h postinvasion (Fig. 3C). When we used SK3842(Δ*hlyE*), the majority of the internalized bacteria remained phagosome bound even after 24 h (Fig. 3D) and some appeared to be partially degraded within the vacuoles (Fig. 3D, arrow). We confirmed the phagosomal escape of SK3842 using a chloroquine resistance assay. Chloroquine accumulates in endosomes and kills endosome-bound bacteria. There was no significant difference in the numbers of CFU of SK3842 recovered from gentamicin-treated cells and from cells treated with both chloroquine and gentamicin (Fig. 3E). This shows that most of the endocytosed SK3842 bacteria escaped rapidly from the endosomes into the host cytoplasm. In contrast, the recovery of SK3842(Δ*hlyE*) was significantly lower in the presence of both chloroquine and gentamicin than in the presence of gentamicin alone, indicating that hemolysin-deficient SK3842 was defective in phagosomal escape. This shows that the expression of the normally cryptic hemolysin gene in SK3842 is one of the major factors responsible for the phagosomal escape of SK3842.

SK3842 is internalized by a microfilament- and microtubule-based phagocytotic pathway. To determine the contributions of host cell signaling and cytoskeletal components to SK3842 internalization, we used a series of chemical inhibitors. Invasion assays were performed in the presence of cytochalasin D (an actin polymerization inhibitor), colchicine (a microtubule polymerization inhibitor), chlorpromazine (an inhibitor of clathrin-mediated endocytosis), nystatin (an inhibitor of endocytosis via lipid rafts), amiloride (a blocker of macropinocytosis), mevastatin (a pan-Rho GTPase inhibitor), genistein (a tyrosine kinase inhibitor), staurosporine (a Ser/Thr kinase inhibitor), and wortmannin (a phosphatidylinositol-3 kinase inhibitor) (Fig. 4A). Cytochalasin D treatment virtually abolished SK3842 invasion, while colchicine reduced SK3842 invasion by 48%, indicating that the internalization of SK3842 is critically dependent on intact host cell microfilaments and to a slightly lesser extent on intact microtubules. Mevastatin and staurosporine strongly inhibited SK3842 entry, indicating that Rho GTPases, which are critical regulators of actin dynamics, and Ser/Thr kinases are crucial for entry of SK3842. Other drugs were ineffective in blocking SK3842 invasion of host cells. Thus, intact actin and microtubules, Rho GTPases, and Ser/Thr protein kinase C are some of the host components involved in SK3842 entry, culminating in an efficient cytoskeletal protein-based phagocytic process.

Curli fibers promote SK3842 internalization. The parental strain MG1655 is a canonical noninvasive organism lacking an apparent invasive apparatus. Therefore, it was important to identify the components of SK3842 that allow host cell entry. Based on SK3842 microarray data (unpublished results), we focused on two possible loci that have been shown to be involved in host cell invasion and showed differential expression from the parental strain, encoding curli fibers (*csg*) and Ivy lysozyme inhibitor (*ivy*) (4, 16, 17). Ivy aids in colonization of specific niches, and curli fibers are involved in host cell adhesion and invasion. We created an *ivy* null mutant by insertion mutagenesis; however, we failed to create a *csg* deletion strain. Instead, we used a synthetic β-breaker peptide (NH_2-QFGGGNPP-COOH; see reference 1) conjugated to a hexapeptide repeat of a major curli fiber protein, CsgA, to disrupt the assembly of curli fibers. Using SK3842(Δ*ivy*) or SK3842 grown in the presence of the breaker peptide, we found that the *ivy* deletion did not impact SK3842 invasion ($P = 0.109$) but curli breaker peptides caused a dose-dependent inhibition (P values of 0.006 and 0.004 for the 0.2 μM and 0.4 μM inhibitor concentrations, respectively) (Fig. 4B). Inclusion of the breaker peptide with SK3842(Δ*ivy*), however, resulted in a further reduction in SK3842 invasion capacity ($P = 0.002$). SK3842(Δ*hlyE*) showed no defect in host cell invasion. This result shows that curli fibers, which are constitutively activated in SK3842, play a major role in host cell invasion and Ivy possibly has a synergistic effect on curli fiber-mediated host cell invasion.

SK3842 replicates efficiently inside the host cell. We estimated the survival and/or replication of strain SK3842 in Int-407 cells by counting gentamicin-resistant intracellular bacteria at various time points after a 1-h infection period (Fig. 4C). The number of intracellular bacteria increased gradually over 14 h, reaching a peak of 300% ± 75% of the bacteria recovered at 1 h. From 14 h to 24 h, there was no appreciable change. This result showed that SK3842, despite being a nontraditional invasive strain, could survive for at least 24 h in the host cell cytoplasm, replicate intracellularly, and resist being killed by the cellular machinery of the invaded cells.

Expression of certain bacterial virulence-associated genes is turned off intracellularly. The Hemolysin E is a cytolytic protein that potentially can destroy host cells. Since SK3842 survived intracellularly and showed no signs of cytotoxicity (see below), we investigated the expression of the *hlyE* gene, along with that of *hupA* and *rrsB*, at various times postinvasion by reverse transcription-PCR (RT-PCR) on total RNA from internalized SK3842 (Fig. 4D). Following SK3842 internalization, there was a sharp decline in *hlyE* expression, from robust expression 1 h postinvasion to complete absence after 24 h; *hupA* expression also showed a progressive decrease over time, but the loss was much less extensive. *rrsB* mRNA levels showed a gradual increase from 1 h to 24 h, consistent with the increase in the number of intracellular SK3842 bacteria. This strong downregulation of a potent cytotoxic gene in SK3842 after the completion of phagosomal escape explains why the mammalian cells remained intact even as the bacterial burden increased.

SK3842 does not induce host cell death. Mammalian cell death by apoptosis or necrosis usually shares some common features, such as chromosomal DNA degradation and loss of membrane integrity. Chromosomal DNA extracted from Int-407 cells infected with different MOIs of SK3842 did not show any signs of fragmentation (Fig. 5A). SK3842-infected cells did not exhibit a significant difference in chromatin fragmentation (Fig. 5B) or lactate dehydrogenase (LDH) activity (Fig. 5C) from that of uninfected cells. SK3842-infected cells stained with Hoechst and propidium iodide (PI) did not show any nuclear condensation or fragmentation or any increase in membrane permeability indicative of apoptosis (Fig. 5D, bottom panel, versus Fig. 5D, middle panel) and showed no qualitative difference from control cells (Fig. 5D, top panel). Immunoblotting of SK3842-infected cell lysates confirmed that there was no cleavage of PARP into the 85-kDa active fragments or cytosolic release of cytochrome *c* for up to 24 h (Fig. 5E). Our results indicate that SK3842 infection does not induce any of the early events of apoptosis, such as cytochrome *c* release and PARP cleavage, or the final apoptotic indicators, such as nucleosomal DNA fragmentation and loss of membrane integrity.

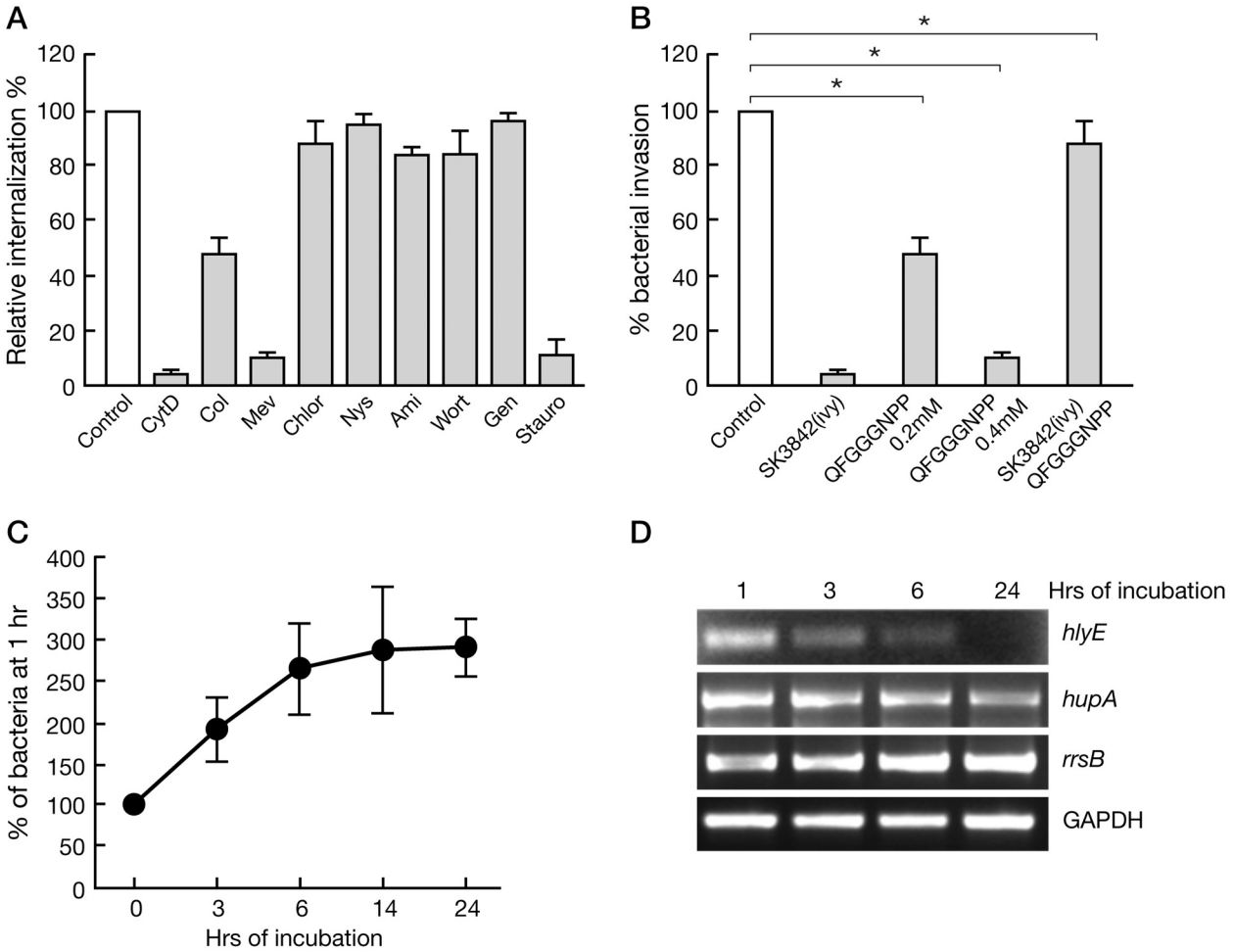

FIG 4 Curli fiber-mediated cell invasion and intracellular replication of SK3842. (A) Effect of chemical inhibitors on SK3842 entry. Int-407 cells were treated with either DMSO (control), cytochalasin D (CytD) (0.5 μM), colchicine (Col) (0.25 μM), mevastatin (Mev) (25 μM), chlorpromazine (chlor) (2 μg/ml), nystatin (Nys) (25 μg/ml), amiloride (Amil) (50 μM), wortmannin (Wort) (200 nM), genistein (Gen) (100 μg/ml), or staurosporine (Stauro) (200 nM) for 2 h, followed by SK3842 infection in the continued presence of the original drug. The viable count was expressed as a percentage of DMSO control (100%). (B) Inhibition of curli fiber formation diminishes invasion. SK3842 cultures grown in the presence and absence of the synthetic peptide NH_2-PPQFGGGNPP-COOH were used to infect Int-407 cells in the continued presence of the peptide. SK3842(Δ*ivy*) was grown on its own or in the presence of NH_2-PPQFGGGNPP-COOH. "*" represents a *P* value of <0.01 compared to results for the control culture. (C) Intracellular replication. Int-407 cells were infected with SK3842 for 1 h, 3 h, 6 h, 14 h, and 24 h. At the conclusion of the infection period, the number of intracellular bacteria was scored and expressed as a percentage of the number of intracellular bacteria recovered after 1 h of infection. (D) Time course of hemolysin gene expression. Total cellular RNA was extracted from SK3842-infected cells at indicated time points. Reverse transcription-PCR amplification with gene-specific primer pairs was done on cDNA transcribed from total RNA. Glyceraldehyde-3-phosphate dehydrogenase (GAPDH) was used as an internal control for equal loading.

Bim phosphorylation and degradation and Puma suppression are two major host cell responses to SK3842 invasion. The BclII family group of proteins, consisting of pro- and antiapoptotic members, contains the principal players determining the fate of a mammalian cell (18). We examined the cellular levels of antiapoptotic multidomain members (Bcl-2, Bcl-XL, and Mcl-1), proapoptotic multidomain proteins (Bax, Bak, and Bok), and proapoptotic BH3-only proteins (Bid, Bad, Puma, and Bim) at different time points following SK3842 invasion. There was no major change in the levels of most BclII group of proteins (Fig. 6A) except for two proapoptotic proteins, Bim_{EL} and Puma. There was a slight but reproducible increase in the antiapoptotic protein Mcl-1 in SK3842-infected cells. The changes in Puma and Bim were much more significant. Puma showed a sharp decline 14 h after infection and was barely detectable at 24 h. We observed an upward electrophoretic mobility shift in both Bim_{EL} and Bim_L (with Bim_{EL} being the predominant isoform), suggestive of increased phosphorylation. Since Bim_{EL} was the most prominent Bim isoform, we focused on it. The electrophoretic shift of Bim_{EL} was also accompanied by a gradual decline in its cellular level. Incubation of SK3842-infected cell lysate with λ-phosphatase (λ-PPase) resulted in the disappearance of the slower-migrating form of Bim_{EL} (Fig. 6B), confirming that the slower-migrating band represented the phosphorylated form of Bim_{EL}. Addition of the λ-PPase inhibitor NaF prevented the appearance of the more rapidly migrating (dephosphorylated) form of Bim_{EL}. Since it has been reported that phosphorylation of Bim_{EL} leads to proteasome-mediated degradation of Bim_{EL}, we used the proteasome inhibitor MG132 to confirm the depletion of phosphorylated Bim_{EL}. Addition of MG132 led to accumulation of both

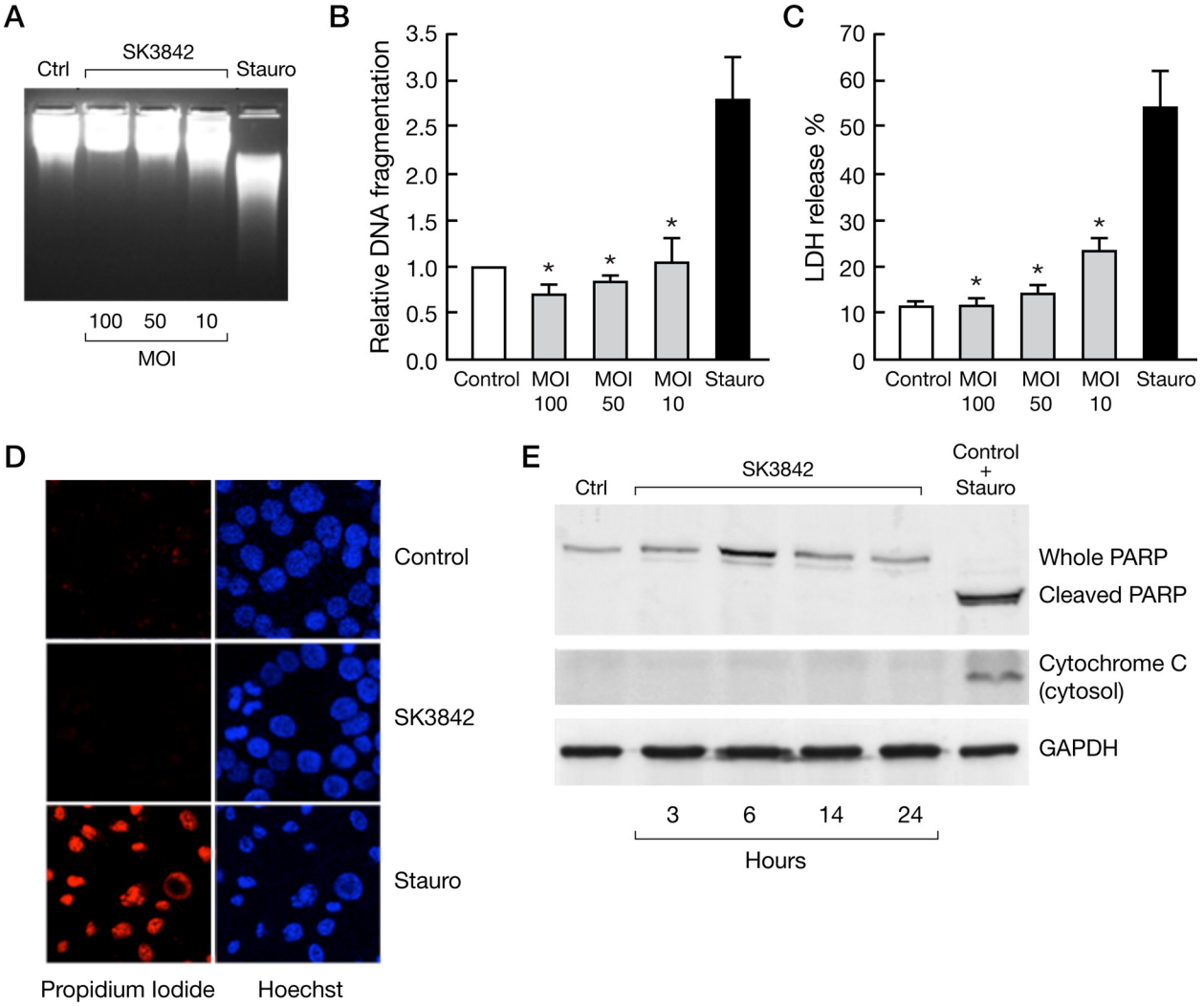

FIG 5 SK3842 infection in epithelial cells does not induce host cell death. (A) DNA degradation in host cells. Chromosomal DNA from uninfected or SK3842-infected Int-407 cells following 24 h of incubation was examined by agarose gel electrophoresis. (B) Quantitation of DNA fragmentation. Cytoplasmic chromatin fragments in uninfected and SK3842-infected cultures following an infection period of 24 h were determined. "*" denotes a *P* value of <0.05 compared to results for staurosporine (Stauro)-treated control cells. (C) Plasma membrane permeabilization. LDH activity in the supernatants of uninfected and SK3842-infected cells following an infection period of 24 h was measured. "*" denotes a *P* value of <0.01 compared to results for staurosporine-treated control cells. (D) Nuclear morphology. Int-407 cells were left uninfected or infected with SK3842 for 24 h. Cells were stained with Hoechst and PI, and representative pictures were taken by a fluorescence microscope. (E) PARP processing and mitochondrial cytochrome *c* release. Int-407 cells infected with SK3842 were collected 3 h, 6 h, 14 h, and 24 h postinfection, lysates were prepared for whole-cell extract (PARP and GAPDH) and the cytosolic fraction (cytochrome *c*), and Western blot analysis was done with PARP, cytochrome *c*, and GAPDH antibodies.

phosphorylated Bim_{EL} and Puma in SK3842-infected cells (Fig. 6C), indicating that both phosphorylated Bim_{EL} and Puma are proteasomally degraded in SK3842-infected cells. These results showed that SK3842 infection leads to major changes in at least 2 principal BH3-only proteins, Bim and Puma.

SK3842 infection confers increased resistance to external apoptotic stimulus. Since SK3842 entry did not result in host cell lethality, we wanted to check whether SK3842 infection could affect host cell susceptibility to external apoptotic signals. Treatment with staurosporine (a potent inducer of cell death) produced a much lower percentage of cells with apoptotic nuclei in SK3842-infected cells than in uninfected cells (Fig. 7A). SK3842-infected cells showed a significant reduction ($P = 0.03$) in staurosporine-induced apoptosis compared to uninfected cells by quantitative cell death enzyme-linked immunosorbent assay (ELISA) (Fig. 7B). There was also a marked reduction in proteolytic cleavage of PARP, caspase 3, and caspase 9, as well as the cytosolic level of cytochrome *c*, in SK3842-infected cells (Fig. 7C). Lower caspase 3 activity was confirmed by the reduced cleavage of Z-Asp-glu-val-asp-7-Amini-4-trifluoromethylcoumarin (Z-DEVD-AFC), a caspase substrate, by SK3842-infected cell lysate compared to that by uninfected cell lysate ($P = 0.01$) (Fig. 7D). These results, taken together, indicate that SK3842 infection inhibits the apoptotic response in host cells challenged with an external cytotoxic stimulus. Uptake of dead SK3842 or latex beads by host cells produced a significant increase ($P = 0.018$ and 0.004, respectively) in staurosporine-induced caspase 3 activity compared to that of live SK3842-infected cells (Fig. 7E). This shows that the inhibition of

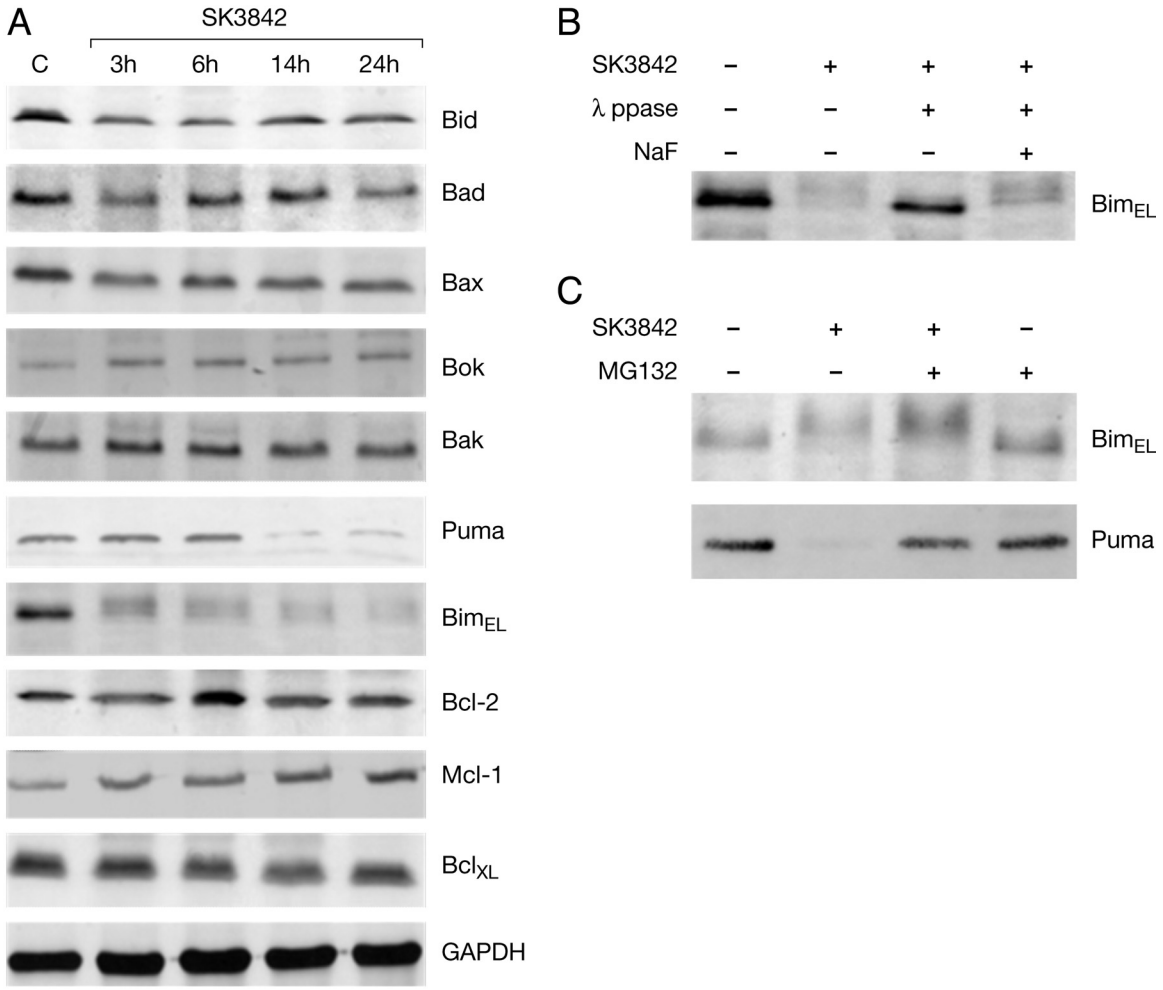

FIG 6 Phosphorylation and degradation of Bim and disappearance of Puma in SK3842-infected cells. (A) Cellular levels of the Bcl-2 family of proteins. Whole-cell extracts of uninfected (first lane) and SK3842-infected cells were collected at the given time points and immunoblotted for both proapoptotic and prosurvival proteins. GAPDH was used as an internal loading control. (B) Bim_{EL} phosphorylation. Western blot analysis of Bim_{EL} from uninfected and 24-h-infected cells minus and plus *in vitro* treatment with λ-phosphatase. The last lane contained cell lysate treated additionally with NaF to deactivate λ-phosphatase. (C) Proteasomal activity degrades Bim_{EL} and Puma. Uninfected and SK3842-infected cells were incubated in the absence and presence of the proteasome inhibitor MG132 and lysates used for immunoblotting with Bim and Puma antibodies.

apoptotic response in host cells requires endocytosis of live SK3842 bacteria. Roles of Bim_{EL} and Puma in mediating increased apoptosis resistance in SK3842-infected cells were tested. Staurosporine treatment of SK3842-infected cells induced dephosphorylation of Bim_{EL} and elevation of the Puma level over that of untreated SK3842-infected cells (Fig. 7F). However, the degree of Bim_{EL} dephosphorylation and the amount of Puma accumulation were still less than those in uninfected staurosporine-treated cells, accounting for the difference in the apoptotic response in these two cell cultures. Staurosporine treatment did not change the Mcl-1 level in uninfected Int-407 cells, implying that depletion of Mcl-1 does not play a major role in staurosporine-induced apoptosis in normal Int-407 cells. However, staurosporine caused an almost complete loss of the Mcl-1 protein in SK3842-infected cells, a finding which was unanticipated.

SK3842 invades intestinal mucosal cells both *in vivo* and *ex vivo* but exhibits no increase in virulence. Given the limitations of cultured cell lines as reliable models for bacterial invasion and to confirm our hypothesis with a more relevant model, we used the murine intestinal ligated loop model and live murine intestinal implants to analyze the interaction of SK3842 with the intestinal mucosa. In the *in vivo* murine ligated intestinal loop assay, bacterial cultures were injected into sutured-off intestinal segments in anesthetized mice. The percentage of the initial bacterial inoculum recovered from intestinal mucosal cells 1 h postinoculation was 7.8% ± 3.6% for SK3842, as opposed to only 0.001% for MG1655 (Table 1). These data are consistent with the *in vitro* data using Int-407 cells. The number of SK3842 bacteria from the intestinal cells increased to 13.4% ± 2.7% after 3 h of inoculation, indicating that the number of internalized bacteria from intestinal mucosal cells not only remained undiminished but also increased marginally. Using an *ex vivo* model of bacterial invasion, we used live intestinal segments from mice to test the invasive capacity of SK3842. SK3842 showed a comparable invasive ability of 17.6% ± 8.6% for the intestinal implant tissue. Thus, the invasive phenotype of SK3842 is not restricted to *in vitro*-cultured cells but is also evident under *in vivo* and *ex vivo* conditions.

We wanted to check whether the invasive ability of SK3842

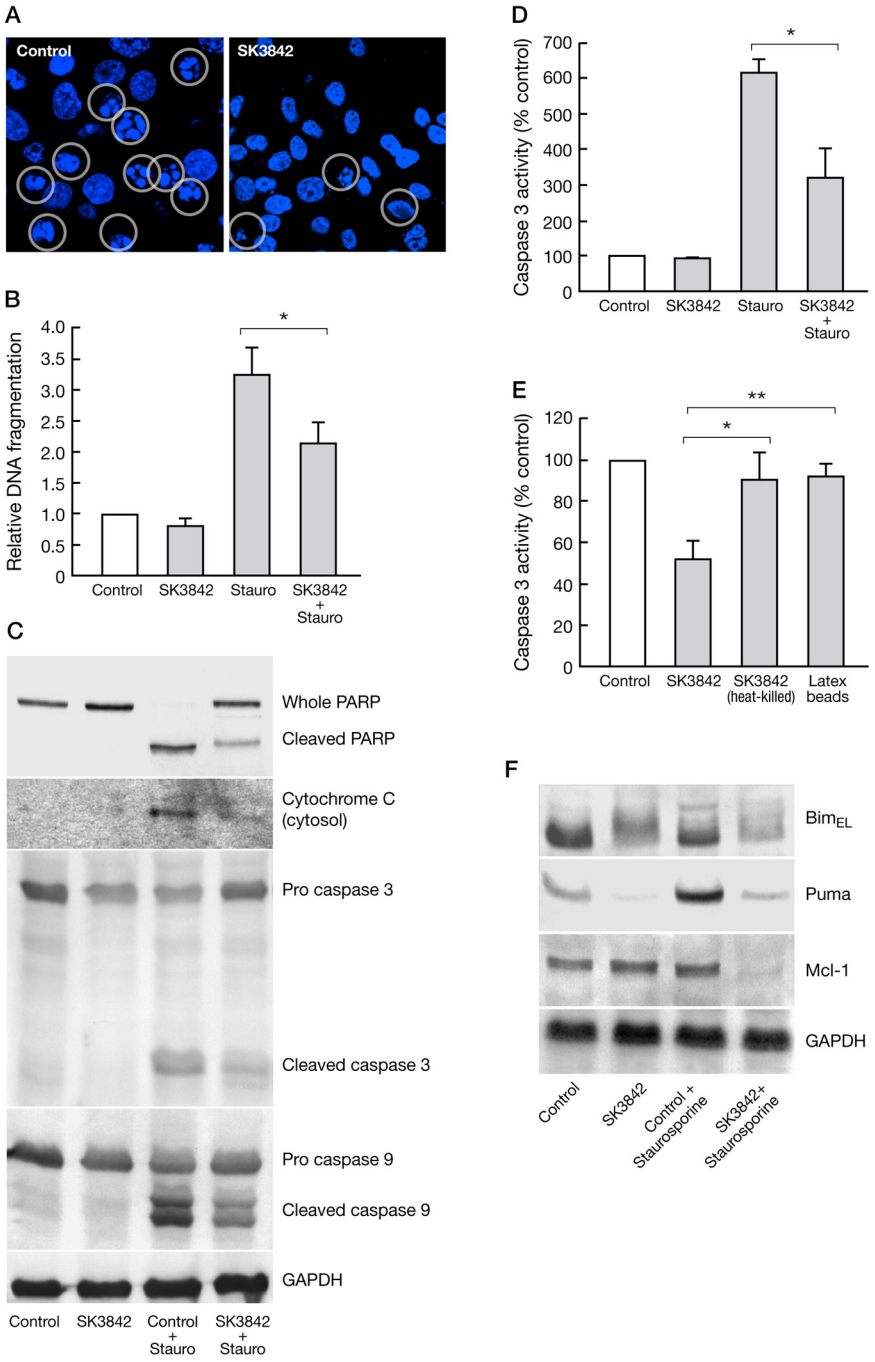

FIG 7 SK3842 confers protection against staurosporine-induced cell death in host cells. (A) Nuclear morphology. Uninfected and SK3842-infected cells were treated with staurosporine, stained with Hoechst stain, and visualized under a fluorescence microscope to score the number of apoptotic nuclei (open circles). (B) Quantitation of DNA fragmentation. Relative apoptosis rates were determined in uninfected and SK3842-infected cells in response to staurosporine by chromatin fragmentation assay. "*" Represents a P value of <0.05 in comparison to results for staurosporine-treated control cells. (C) Status of principal apoptosis marker proteins. Cleavage of PARP, caspase 3, and caspase 9 and release of mitochondrial cytochrome *c* into the cytosol were determined in uninfected and SK3842-infected cells treated with staurosporine. Whole-cell extracts or cytosolic fractions were prepared and used for immunoblotting with the indicated antibodies. (D) Caspase 3 activity. The effect of SK3842 infection on caspase 3 activity was measured with DEVD-AFC as a substrate using lysates from uninfected and SK3842-infected cells treated with staurosporine. "*" Denotes a P value of <0.05 compared to results for staurosporine-treated control cells. (E) Effect of phagocytosis of killed SK3842 and latex beads on cytoprotection. Effect of heat-killed SK3842 (MOI of 100) and latex bead (1.1 μM) phagocytosis on staurosporine-induced caspase activation in Int-407 cells. After 24 h, cells were treated with staurosporine and lysed for measurement of caspase 3 activity using DEVD-AFC as a substrate. "*' denotes a P value of <0.05, and "**" denotes a P value of <0.01. (F) Effect on BclII proteins upon staurosporine treatment. Cell lysates from staurosporine-treated uninfected and SK3842-infected cells were used for immunoblotting with Bim, Puma, and Mcl-1 antibodies.

TABLE 1 Invasion of intestinal epithelial cells *in vivo* and *ex vivo* by SK3842

Strain	% of invasion[a]			
	In vivo[b]			
	1 h	3 h	*Ex vivo*[c]	LD_{50}
SK3842	7.8 ± 3.6	13.4 ± 2.7	17.6 ± 8.6	1.6×10^8
MG1655	0.001	0.002	0.004	2.1×10^8

[a] Percentage of bacteria in the inoculum that invaded intestinal mucosal cells.
[b] Invasion assay done as per the ligated intestinal loop assay described in Materials and Methods.
[c] Invasion assay done as per *ex vivo* intestinal invasion assay described in Materials and Methods.

resulted in greater virulence in a mouse model. The 50% lethal dose (LD_{50}) of MG1655 for intraperitoneal (i.p.) inoculation was 2.1×10^8 and was consistent with earlier observations about the virulence index of *E. coli* K-12. The LD_{50} of SK3842 was comparable at 1.6×10^8 (Table 1), showing that the transition from an extracellular to an invasive form does not lead to enhanced lethality of SK3842.

DISCUSSION

Invasion of host cells is often the first step adopted by many pathogenic bacteria to initiate their virulence process. However, except for the small subset of enteroinvasive *E. coli* strains, host cell invasion is not a preferred mode of interaction by even pathogenic *E. coli* (19). We previously showed that an HU mutant *E. coli* laboratory strain, SK3842, expresses many silent pathogenesis-linked genes (12). We also demonstrated that the $HU\alpha^{E38K,\ V42L}$ mutant generates positive superhelicity while wild-type HU creates negative supercoiling both *in vitro* and *in vivo* (13). The results reported here showing that the *hlyE* promoter retains its active status in plasmids isolated from SK3842 and remains responsive only to $HU\alpha^{E38K,\ V42L}$ and not to wild-type HUα confirm that $HU\alpha^{E38K,\ V42L}$ modulates the physical architecture of promoters of cryptic, pathogenicity-related genes. This is consistent with the model of positive supercoiling generated by $HU\alpha^{E38K,\ V42L}$, most likely in a segmental fashion, which allows transcription of these pathogenesis-associated genes. These promoters are silent when DNA is negatively supercoiled, as in the wild-type cell. The change in physical and biochemical attributes of the E38K V42L mutation were previously shown to correlate with widespread morphological and physiological changes in SK3842. In this present study, we have demonstrated that the cellular changes resulting from $HU\alpha^{E38K,\ V42L}$ are responsible for a major shift in traditional *E. coli* K-12–epithelial cell interaction dynamics: from a strictly extracellular, noninvasive behavior, SK3842 adopts an efficient intracellular mode of existence. Entry and postinternalization events of SK3842 follow many of the archetypal maneuvers of such invasive pathogens as *Shigella* and *Salmonella*: (i) epithelial cell entry by actin-based invasion, (ii) phagosomal escape, and (iii) intracellular replication (20). Activation of at least two major, normally quiescent virulence determinants is responsible for this invasive phenotype: curli fibers for host cell entry and hemolysin E for phagosomal escape. Hemolysin E expression is strongly repressed following the phagosomal escape of SK3842, indicating an active bacterial strategy to limit cytotoxicity intracellularly. Abolition of the invasive phenotype with reversion of SK3842 to its wild-type form proved that SK3842 behavioral changes are directly linked to its mutant physiological characteristics and not induced by any unrelated genomic alterations. Functional divergence from the canonical host-microbe interaction, without any gross genotypic variation, has been reported in some cases (21, 22). But to our knowledge this is the first instance where mutation in an architectural protein has resulted in an extracellular commensal bacterial species adopting an invasive phenotype. Others have shown that ectopic overexpression of curli fibers triggers host cell entry (16) and overexpression of hemolysin E imparts a hemolytic phenotype to *E. coli* K-12 (23). This indicates that despite their functional inconsequence under normal conditions, these genes encode proteins with valid physiological effects and possibly fulfill certain indispensable cellular demands during atypical situations. The present study provides an empirical linkage between global nucleoid remodeling-linked physiological changes in *E. coli* K-12 and a functional shift in behavioral pattern with regard to host cells. There are known bacterial architectural proteins, like H-NS in the enterobacteriaceae and Lsr2 in *Mycobacterium* (24–26), which undergo structural and functional changes in response to host cues and act as master switches to manipulate bacterial virulence by changing the global gene expression profile. It is possible that HU, the most abundant and well-conserved bacterial architectural protein, can also assume different structural configurations in response to specific host environmental cues, and the $HU\alpha^{E38K,\ V42L}$ protein conformation and resultant cellular changes are representative of the host-induced changes in a select residential bacterial population.

Delay or prevention of epithelial cell apoptosis after bacterial infection allows invading bacteria time to adapt to the intracellular environment before invading deeper mucosal layers and to maintain their residential niche (27). Invasion by SK3842 does not trigger host cell death—a phenomenon which is perhaps imperative for SK3842's survival and intracellular replication. SK3842 infection also confers significant apoptosis resistance against external apoptotic stimuli, such as staurosporine. Two critical cellular events underlying the SK3842-infected host cell survival are phosphorylation-driven Bim_{EL} degradation and downregulation of Puma. Of all the BH3-only proteins, only Bim and Puma (along with t-Bid) can engage with and antagonize every single prosurvival Bcl-2 molecule (28). Loss of Bim and Puma renders cells resistant to chemotherapy drugs, gamma irradiation, and cytokine deprivation (29). Bim and Puma have also been shown to be involved in apoptosis resistance in host cells harboring such obligate intracellular microbes as *Chlamydia* (30). The fact that SK3842 infection degrades two of the most potent, multispecificity prodeath proteins probably accounts for the fact that infected host cells do not display any sign of cell death even after 24 h and up to 96 h (data not shown). This is not the case for traditional invasive bacteria, such as *Salmonella* and *Shigella*, which cause apoptosis of the host epithelial cells after a delay of 12 to 18 h (31). One of the major prosurvival proteins, Mcl-1, also shows a slight upregulation in SK3842-infected cells. Mcl-1 interacts with a high affinity to the BH3-only proteins Bim, Puma, and Bid but also selectively interacts with the "effector" proapoptotic protein Bak (32). The major prosurvival role of Mcl-1 is postulated to be linked to its sequestration of Bak on the outer mitochondrial membrane, preventing Bak oligomerization. In SK3842-infected cells, Bim and Puma are not available for interaction due to their phosphorylation status and/or disappearance. Therefore, a much

larger pool of Mcl-1 is available to sequester Bak from initiating apoptosis. The increased available Mcl-1 pool coupled with the slight increase in its cellular level is probably responsible for the improved apoptosis resistance of SK3842-infected cells. Upon staurosporine treatment of SK3842-infected cells, increased levels of unphosphorylated Bim and Puma disrupt the Mcl-1–Bak interaction and unleash Bak for initiation of the apoptosis cascade. But since the levels of Bim and Puma are still much lower than those in uninfected, staurosporine-treated cells, these cells showed lower indices of apoptosis. One paradoxical observation was the complete abrogation of the Mcl-1 level in staurosporine-treated SK3842-infected cells. We are not sure of the reason for this phenomenon, but it is possible that the proteasomal degradation system is more active in SK842-infected cells and that Mcl-1, untethered from its binding partner Bak, is subjected to much more rapid degradation than in normal cells. Invasiveness is a trait almost uniquely associated with pathogens and host cell lethality. The fact that SK3842 engenders a well-defined survival program in the host cell and shows no increase in virulence in an animal model signifies that SK3842 not only is an unconventional derivative of extracellular *E. coli* but also follows a noncanonical intracellular relationship with the host cell.

Apart from enteroinvasive *E. coli*, there have been reports of even other *E. coli* pathovars exhibiting invasive behavior under *in vitro* conditions. Enteroaggregative and enteropathogenic strains have been reported to invade intestinal epithelial cells *in vitro* (33, 34). However, these strains do not show intracellular replication and phagosomal escape or invade human intestinal explants *in vivo* (35) and thus do not appear to be specifically adapted for intracellular survival. In contrast, SK3842 not only exhibits classical invasive properties *in vitro* but also retains its invasive phenotype under *in vivo* (ileal loop assay) and *ex vivo* (intestinal explants assay) conditions, indicating that its invasive trait is an integral cellular attribute and hence is of possible physiological significance. Not all invasive *E. coli* strains require dedicated invasive machinery. Adhesive-invasive *E. coli* (AIEC), associated with the genesis of Crohn's disease, shows invasive properties similar to those of SK3842 (36). AIEC strains also lack specific virulence determinants, and the genes which have been implicated in AIEC pathogenesis are present in commensal K-12 strains, giving rise to the idea that only changes in the gene expression profile or minor sequence variations in commensal *E. coli* strains generate the virulence potential of AIEC strains (37). SK3842 is morphologically and physiologically completely distinct from AIEC strains, probably reflecting the fact that there are diverse modes and consequences of extracellular *E. coli* adopting an invasive lifestyle in the absence of any external genetic flux. Further work using SK3842 as (i) an *in vitro* model to study the molecular events associated with a change in mammalian cell–*E. coli* K-12 interaction and (ii) a traceable *in vivo* model for analyzing commensal bacteria in invasive modes can provide valuable insights into host-microbe dynamics and potential routes of divergence from the canonical code.

MATERIALS AND METHODS

Bacterial strains and cell line. SK3842 and its growth conditions have been described previously (12). MG1655(Δ*hlyE*) and MG1655(Δ*ivy*) were created by inserting a *cat* cassette within the *hlyE* gene and a *kan* cassette within the *ivy* gene by recombineering using the method of Yu et al. (38). Primers used for these experiments were as follows: for MG1655(Δ*hlyE*), GAGGCGAATGATTATGACTGAAATCGTTGCAGA TAAAACGGTAGAAGTAGTTAAAAACGCAATCGTGTGACGGAAGA TCACTTCG (forward primer) and TCAGACTTCAGGTACCTCAAAGA GTGTCTTTTTACCGTGTCTTTTCTGATACTCATTACACCAGCAAT AGACATAAGCG (reverse primer); and for MG1655(Δ*ivy*), GGAGGTT AATAACATGGGCAGGATAAGCTCGGGAGGAATGATGTTTAAGG CTATGGACAGCAAGCGAACCG (forward primer) and TTATTTAAA ATTAAAGCCATCCGGATGGTTTTCCAGGCTGCCGGTCAACGCTC AGAAGAACTCGTCAAGAAG (reverse primer). The mutant HUα gene was transduced into these two strains by P1 transduction to convert them to SK3842(Δ*hlyE*) and SK3842(Δ*ivy*). DMO100 (MG1655 Δ*hupAB*) has been described previously (39). To make the *in vitro* transcription plasmid for *hlyE*, plasmid SK302(*hlyE*) was constructed by cloning a fragment of DNA stretching from −474 bp to +82 bp relative to the *hlyE* transcript start site at the EcoRI-HindIII sites of the pBR322 vector. SK761(*lac*) was constructed by cloning 390 bp of the *lac* promoter (−314 to +76) into the EcoRI and PstI sites of the transcriptional vector pSA508 (40). The Int-407 cell line (human embryonic intestine; ATCC CCL 6) was obtained from the American Type Culture Collection. This cell line was maintained in Dulbecco's modified Eagle's medium (DMEM) supplemented with 10% fetal bovine serum, 2 mm glutamine, and 100 U/ml penicillin-streptomycin in a humidified incubator in an atmosphere of 10% CO_2 at 37°C.

Quantitative invasion assay. Invasion efficiency was tested by a gentamicin protection assay as per established protocol. Int-407 cells were infected with SK3842 at different MOIs for 1 h, followed by the addition gentamicin-containing culture medium (100 μg/ml). At various times postinfection, cells were washed and lysed with phosphate-buffered saline (PBS) containing 0.5% Triton X-100. Appropriate dilutions of the lysed solution were plated on agar plates, and the number of viable bacteria was determined. Unless mentioned otherwise, the MOI used was 1:100, infection time was for 1 h prior to incubation in gentamicin-DMEM, and incubation time was 24 h following 1 h of infection. The MOI used for MG1655 and LT2 was 1:100.

Chloroquine resistance assay. Phagosomal escape was evaluated with a chloroquine resistance assay (41). Briefly, infected Int-407 cells were incubated in the presence of gentamicin (100 μg/ml) with or without chloroquine (100 μg/ml) for an additional 5 h. The cells were subsequently lysed and plated to determine the number of intracellular bacteria surviving the drug treatment.

Transcription assays. For *in vitro* transcription of *lacP*, supercoiled DNA template (2 nM) was preincubated with or without proteins at 37°C in a 45-μl reaction mixture containing 20 mM Tris acetate (pH 7.8), 10 mM magnesium acetate, 100 mM potassium glutamate, 1 mM ATP, and 1 mM dithiothreitol (DTT). When needed, 0.1 mM cAMP, 50 nM CRP, and either 160 nM HUα or $HU^{\alpha E38K,\ V42L}$ were added before the addition of 20 nM RNA polymerase. After incubation for 5 min, transcription was initiated by the addition of 5 μl of NTP mix containing 0.1 mM GTP, 0.1 mM CTP, 0.01 mM UTP, and 20 μCi of [α-32P]UTP (3,000 Ci/mmol) (ICN). Reactions were terminated after 10 min by addition of an equal volume of RNA loading buffer (80% [vol/vol] deionized formamide, 1× Tris-borate-EDTA [TBE], 0.025% bromophenol blue, 0.025% xylene cyanol). The reactions were analyzed on an 8% polyacrylamide-urea gel followed by autoradiography. When required, 160 nM HUα or $HU^{\alpha E38K,\ V42L}$ was added before RNA polymerase. For *hlyE* transcription, S-30 extract from DM0100 was prepared according to the method of Zubay (42). Standard S-30 transcription reactions were carried out in a final volume of 50 μl, and reaction mixtures contained Tris acetate (20 mM, pH 8.0), magnesium acetate (10 mM), potassium glutamate (300 mM), ammonium acetate (30 mM), DTT (1 mM), 5 U RNasin, ATP (2 mM), CTP (0.5 mm), GTP (0.5 mm), and UTP (0.05 mM) added in a 2.5× master mix. Three hundred nanomolar HUα or $HU^{\alpha E38K,\ V42L}$ and 360 μg of the S-30 protein in 15 μl were added to 20 μl of concentrated master mix. After preincubation on ice for 30 min, 30 nM plasmid DNA, isolated from either MG1655 or SK3842, was added to the reaction mix. After 10 min of incubation at 37°C, 20 μCi of [α-

32P]UTP (ICN, 1,000 to 3,000 Ci/mmol) was added to the reaction mixture. Reactions were stopped after 10 min by the addition of 0.6 volume of phenol. After phenol extraction (1×) followed by chloroform extraction (1×), samples were ethanol precipitated and the pellets were suspended in 10 μl Tris-EDTA buffer. Five-microliter-aliquot samples were heated, chilled, and run on an 8% sequencing gel, followed by autoradiography.

RT-PCR. RT-PCR and the gene-specific primers have been described before (12).

Apoptosis assays. The LDH assay was carried out with the colorimetric CytoTox 96 assay kit (Promega), following the instructions of the manufacturers. The data obtained were expressed as percent LDH release relative to total LDH in culture. Quantitative DNA fragmentation was determined by an enzyme-linked immunoassay kit (cell death detection ELISA^{plus}; Roche) to detect fragmented DNA and histones (mononucleosomes and oligonucleosomes), following the instructions of the manufacturers. DNA fragmentation assays were done by harvesting infected and noninfected cells (2×10^5), followed by suspension in 300 μl lysis buffer containing 10 mM Tris (pH 7.8), 5 mM EDTA, and 0.5% SDS and incubation at 65°C for 60 min. Lysates were then treated with RNase A (20 μg/ml, 37°C, 1 h) and proteinase K (20 μg/ml, 50°C, 1 h) and extracted twice with an equal volume of phenol-chloroform. DNA was then precipitated at −20°C with 0.3 M sodium acetate–95% ethanol. Precipitated DNA was dissolved in 30 μl of Tris-EDTA buffer and subjected to electrophoresis on a 2% agarose gel containing ethidium bromide.

Protein isolation and Western blotting. Whole-cell extracts were prepared by scraping and collecting cells and washing with ice-cold PBS. Cells were lysed, lysates were centrifuged, and supernatants were collected. For cytochrome *c* release, cells were harvested, washed, and lysed in ice-cold buffer M (20 mm HEPES [pH 7.5], 10 mm KCl, 1.5 mm $MgCl_2$, 1 mm EGTA, 1 mm EDTA, 1 mm DTT, 250 mm sucrose, 0.1 mm phenylmethylsulfonyl fluoride [PMSF], 2 μg/ml pepstatin, 2 μg/ml leupeptin, and 2 μg/ml aprotinin) by homogenization in a small glass homogenizer with a Teflon pestle. The homogenates were centrifuged, and the supernatants were collected. Equal amounts of whole-cell extracts or mitochondrion-free cytosolic fractions were used for Western blotting. Bands were visualized using the Western Lightning chemiluminescence system (NEN-Perkins Elmer) or nitroblue tetrazolium–5-bromo-4-chloro-3-indolylphosphate (NBT-BCIP) (Invitrogen). λ-phosphatase treatment was done at 200 U/20 μg for 1 h at 30°C. The concentration of NaF used to deactivate λ-phosphatase was 5 mM. Treatment of proteasome inhibitor MG132 was done at a concentration of 25 μM for 8 h.

Determination of LD_{50}. Female 7-week-old BALB/c mice were inoculated i.p. with 100 μl of the bacterial suspension. To determine the 50% lethal dose (LD_{50}), five groups of five mice/group were inoculated i.p. with serial dilutions of bacteria ranging from 10^4 to 10^{10}. Mice were monitored twice daily for 5 days, and the LD_{50} was calculated according to the method of Reed and Muench (43).

Ligated intestinal loop assay. MG1655 and SK3842 (with isogenic spectinomycin markers) cultures were used in a murine intestinal loop assay as per the procedure described elsewhere (44). Six- to 8-week-old BALB/c mice were used for this assay. Groups of five mice were starved for 4 h, after which mice were anesthetized with sodium pentobarbital at a dose of 50 to 67 mg/kg of body weight. A small incision was made through the abdominal wall, and the small intestine was exposed in the anesthetized mice. A 5-cm ileal loop was made at the ileocecal junction and 4 to 5 cm proximal to the ileocecal junction for each mouse. Each ligated loop contained at least one Peyer's patch. A 100-μl volume of bacterial suspension (in normal saline) containing 10^8 CFU was injected into the closed loop. The bowel was returned to the abdominal cavity, and the incision was closed. The mice were kept under anesthesia for 1 to 3 h before they were killed by cervical dislocation. The abdomen was reopened, and the ligated intestines were removed and cut open. Tissue specimens were thoroughly washed with sterile PBS to eliminate mucus and debris and then soaked for 3 h at 37°C in a gentamicin solution (200 μg/ml). The tissue specimens were washed twice with ice-cold PBS to eliminate residual gentamicin and then homogenized in 500 μl of 0.5% Triton X-100, and bacterial titers were determined by plating 100 μl of homogenates on LB-spectinomycin agar plates.

***Ex vivo* intestinal invasion assay.** *Ex vivo* invasion assays were conducted with MG1655 and SK3842 (with spectinomycin markers) cultures using a procedure described elsewhere (45). Groups of five BALB/c mice were deprived of food for 24 h, after which they were euthanized and the small intestines were removed and placed in DMEM-fetal bovine serum (FBS). One-inch sections were cut from the ileal region, and the lumen was thoroughly washed with 1× PBS. One end was tied off, and 100 μl of bacterial culture containing 10^8 CFU was injected into the intestinal section. The other end was tied off, and the tissue was placed in DMEM-FBS and allowed to incubate for 1 h at 37°C. The ends were then cut, and the tissue was washed with gentamicin in DMEM-FBS (200 μg/ml). After washing, the intestine was opened longitudinally and allowed to incubate in gentamicin-DMEM-FBS for 1 h at 37°C. The intestinal tissue was then washed three times to remove all traces of gentamicin, homogenized in 2 ml of 0.5% Triton X-100, diluted, and plated on LB-spectinomycin plates.

ACKNOWLEDGMENT

This research was supported in part by the Intramural Research Program of the NIH, National Cancer Institute, Center for Cancer Research, and in part by the Department of Biotechnology, Government of India (BT/PR11351/30/137/2008).

REFERENCES

1. **Cherny I, et al.** 2005. The formation of *Escherichia coli* curli amyloid fibrils is mediated by prion-like peptide repeats. J. Mol. Biol. **352**:245–252.
2. **Anderson JC, Clarke EJ, Arkin AP, Voigt CA.** 2006. Environmentally controlled invasion of cancer cells by engineered bacteria. J. Mol. Biol. **355**:619–627.
3. **Khan MA, Isaacson RE.** 1998. *In vivo* expression of the beta-glucoside (bgl) operon of *Escherichia coli* occurs in mouse liver. J. Bacteriol. **180**:4746–4749.
4. **Bokranz W, Wang X, Tschape H, Romling U.** 2005. Expression of cellulose and curli fimbriae by *Escherichia coli* isolated from the gastrointestinal tract. J. Med. Microbiol. **54**:1171–1182.
5. **Kerényi M, et al.** 2005. Occurrence of hlyA and sheA genes in extraintestinal *Escherichia coli* strains. J. Clin. Microbiol. **43**:2965–2968.
6. **Le Gall T, et al.** 2007. Extraintestinal virulence is a coincidental by-product of commensalism in B2 phylogenetic group *Escherichia coli* strains. Mol. Biol. Evol. **24**:2373–2384.
7. **Rolhion N, Darfeuille-Michaud A.** 2007. Adherent-invasive *Escherichia coli* in inflammatory bowel disease. Inflamm. Bowel Dis. **13**:1277–1283.
8. **Macutkiewicz C, et al.** 2008. Characterisation of *Escherichia coli* strains involved in transcytosis across gut epithelial cells exposed to metabolic and inflammatory stress. Microbes Infect. **10**:424–431.
9. **Guenther K, Straube E, Pfister W, Guenther A, Huebler A.** 2010. Sever [sic] sepsis after probiotic treatment with *Escherichia coli* NISSLE 1917. Pediatr. Infect. Dis. J. **29**:188–189.
10. **O'Boyle CJ, et al.** 1998. Microbiology of bacterial translocation in humans. Gut **42**:29–35.
11. **MacFie J, et al.** 1999. Gut origin of sepsis: a prospective study investigating associations between bacterial translocation, gastric microflora, and septic morbidity. Gut **45**:223–228.
12. **Kar S, Edgar R, Adhya S.** 2005. Nucleoid remodeling by an altered HU protein: reorganization of the transcription program. Proc. Natl. Acad. Sci. U. S. A. **102**:16397–16402.
13. **Kar S, et al.** 2006. Right-handed DNA supercoiling by an octameric form of histone-like protein HU: modulation of cellular transcription. J. Biol. Chem. **281**:40144–40153.
14. **Guo F, Adhya S.** 2007. Spiral structure of *Escherichia coli* HUalphabeta provides foundation for DNA supercoiling. Proc. Natl. Acad. Sci. U. S. A. **104**:4309–4314.
15. **Lim HM, Lewis DE, Lee HJ, Liu M, Adhya S.** 2003. Effect of varying the supercoiling of DNA on transcription and its regulation. Biochemistry **42**:10718–10725.
16. **Gophna U, et al.** 2001. Curli fibers mediate internalization of *Escherichia coli* by eukaryotic cells. Infect. Immun. **69**:2659–2665.

17. **Deckers D, Vanlint D, Callewaert L, Aertsen A, Michiels CW.** 2008. Role of the lysozyme inhibitor Ivy in growth or survival of *Escherichia coli* and *Pseudomonas aeruginosa* bacteria in hen egg white and in human saliva and breast milk. Appl. Environ. Microbiol. **74**:4434–4439.
18. **Chipuk JE, Moldoveanu T, Llambi F, Parsons MJ, Green DR.** 2010. The BCL-2 family reunion. Mol. Cell **37**:299–310.
19. **Nataro JP, Kaper JB.** 1998. Diarrheagenic *Escherichia coli*. Clin. Microbiol. Rev. **11**:142–201.
20. **Parsot C, Sansonetti PJ.** 1996. Invasion and the pathogenesis of *Shigella* infections. Curr. Top. Microbiol. Immunol. **209**:25–42.
21. **Kaern M, Elston TC, Blake WJ, Collins JJ.** 2005. Stochasticity in gene expression: from theories to phenotypes. Nat. Rev. Genet. **6**:451–464.
22. **Osborne SE, et al.** 2009. Pathogenic adaptation of intracellular bacteria by rewiring a cis-regulatory input function. Proc. Natl. Acad. Sci. U. S. A. **106**:3982–3987.
23. **Lai XH, et al.** 2000. Cytocidal and apoptotic effects of the ClyA protein from *Escherichia coli* on primary and cultured monocytes and macrophages. Infect. Immun. **68**:4363–4367.
24. **Blot N, Mavathur R, Geertz M, Travers A, Muskhelishvili G.** 2006. Homeostatic regulation of supercoiling sensitivity coordinates transcription of the bacterial genome. EMBO Rep. **7**:710–715.
25. **Arold ST, Leonard PG, Parkinson GN, Ladbury JE.** 2010. H-NS forms a superhelical protein scaffold for DNA condensation. Proc. Natl. Acad. Sci. U. S. A. **107**:15728–15732.
26. **Gordon BR, et al.** 2010. Lsr2 is a nucleoid-associated protein that targets AT-rich sequences and virulence genes in *Mycobacterium tuberculosis*. Proc. Natl. Acad. Sci. U. S. A. **107**:5154–5159.
27. **Labbé K, Saleh M.** 2008. Cell death in the host response to infection. Cell Death Differ. **15**:1339–1349.
28. **Adams JM, Cory S.** 2007. The Bcl-2 apoptotic switch in cancer development and therapy. Oncogene **26**:1324–1337.
29. **Willis SN, Adams JM.** 2005. Life in the balance: how BH3-only proteins induce apoptosis. Curr. Opin. Cell Biol. **17**:617–625.
30. **Fischer SF, et al.** 2004. *Chlamydia* inhibit host cell apoptosis by degradation of proapoptotic BH3-only proteins. J. Exp. Med. **200**:905–916.
31. **Kim JM, et al.** 1998. Apoptosis of human intestinal epithelial cells after bacterial invasion. J. Clin. Invest. **102**:1815–1823.
32. **Willis SN, et al.** 2005. Proapoptotic Bak is sequestered by Mcl-1 and Bcl-xL, but not Bcl-2, until displaced by BH3-only proteins. Genes Dev. **19**:1294–1305.
33. **Miliotis MD, Koornhof HJ, Phillips JI.** 1989. Invasive potential of noncytotoxic enteropathogenic *Escherichia coli* in an *in vitro* Henle 407 cell model. Infect. Immun. **57**:1928–1935.
34. **Benjamin P, Federman M, Wanke CA.** 1995. Characterization of an invasive phenotype associated with enteroaggregative *Escherichia coli*. Infect. Immun. **63**:3417–3421.
35. **Hicks S, Candy DC, Phillips AD.** 1996. Adhesion of enteroaggregative *Escherichia coli* to pediatric intestinal mucosa *in vitro*. Infect. Immun. **64**:4751–4760.
36. **Boudeau J, Glasser A-L, Masseret E, Joly B, Darfeuille-Michaud A.** 1999. Invasive ability of an *Escherichia coli* strain isolated from the ileal mucosa of a patient with Crohn's disease. Infect. Immun. **67**:4499–4509.
37. **Martinez-Medina M, et al.** 2009. Similarity and divergence among adherent-invasive *Escherichia coli* and extraintestinal pathogenic *E. coli* strains. J. Clin. Microbiol. **47**:3968–3979.
38. **Yu D, et al.** 2000. An efficient recombination system for chromosome engineering in *Escherichia coli*. Proc. Natl. Acad. Sci. U. S. A. **97**:5978–5983.
39. **Lewis DEA, Geanacopoulos M, Adhya S.** 1999. Roles of HU and DNA supercoiling in transcription repression: specialized nucleoprotein repression complex at gal promoters in *Escherichia coli*. Mol. Microbiol. **31**:451–462.
40. **Choy HE, Adhya S.** 1993. RNA polymerase idling and clearance in gal promoters: use of supercoiled minicircle DNA template made *in vivo*. Proc. Natl. Acad. Sci. U. S. A. **90**:472–476.
41. **Paetzold S, Lourido S, Raupach B, Zychlinsky A.** 2007. *Shigella flexneri* phagosomal escape is independent of invasion. Infect. Immun. **75**:4826–4830.
42. **Zubay G.** 1973. *In vitro* synthesis of protein in microbial systems. Annu. Rev. Genet. **7**:267–287.
43. **Reed LJ, Muench H.** 1938. A simple method of estimating fifty percent end points. Am. J. Hyg. **27**:493–497.
44. **Secott TE, Lin TL, Wu CC.** 2004. *Mycobacterium avium* subsp. paratuberculosis fibronectin attachment protein facilitates M-cell targeting and invasion through a fibronectin bridge with host integrins. Infect. Immun. **72**:3724–3732.
45. **Prouty AM, Gunn JS.** 2000. *Salmonella enterica* serovar Typhimurium invasion is repressed in presence of bile. Infect. Immun. **68**:6763–6769.